Segunda cita: teoría KAM

Alejandro Luque

DDays 2014, Badajoz.

14 octubre, 2014

Han pasado unos 60 años desde los primeros trabajos en Teoría KAM (A. K. Kolmogorov, V. I. Arnold, J. K. Moser).

El campo sigue muy abierto en la actualidad. Queda mucho trabajo por hacer, muchas preguntas por contestar y muchas más preguntas por hacer.

También disponemos de más técnicas a nuestra disposición y tenemos una nueva (ejem! 15 años) generación de teoremas basados en el método de la parametrización que puede ser explotada con el uso combinado de ordenadores.

Esto es gracias a caminar sobre hombros de gigantes:
R. de la Llave, A. González, À. Jorba, J. Villanueva, E. Fontich, Y. Sire, G. Huguet, R. C. Calleja, A. Celletti, etc

Han pasado unos 60 años desde los primeros trabajos en Teoría KAM (A. K. Kolmogorov, V. I. Arnold, J. K. Moser).

El campo sigue muy abierto en la actualidad. Queda mucho trabajo por hacer, muchas preguntas por contestar y muchas más preguntas por hacer.

También disponemos de más técnicas a nuestra disposición y tenemos una nueva (ejem! 15 años) generación de teoremas basados en el método de la parametrización que puede ser explotada con el uso combinado de ordenadores.

Esto es gracias a caminar sobre hombros de gigantes:
R. de la Llave, A. González, À. Jorba, J. Villanueva, E. Fontich, Y. Sire, G. Huguet, R. C. Calleja, A. Celletti, etc

Notation:

- Let $\mathbb{T}^n = \mathbb{R}^n/\mathbb{Z}^n$ be the n-dimensional torus with covering space $\mathbb{R}^n$.
- Let $\mathcal{A} \subset \mathbb{T}^n \times \mathbb{R}^n$ be an annulus. The coordinates on $\mathcal{A}$ are denoted by $z = (z_1, \ldots, z_{2n}) = (x, y)$, with $x = (x_1, \ldots, x_n)$ and $y = (y_1, \ldots, y_n)$.
- $\mathcal{A}$ is endowed with an exact symplectic form $\boldsymbol{\omega} = \mathrm{d}\boldsymbol{\alpha}$. In coordinates:

$$a(z) = (a_1(z), \ldots, a_{2n}(z))^\top, \qquad \Omega(z) = \mathrm{D}a(z)^\top - \mathrm{D}a(z).$$

- $\mathcal{A}$ may be endowed with a metric $\boldsymbol{g}$ represented by $G(z)$.

- A manifold $\mathcal{K}$, parameterized by K, is invariant if

$$F \circ K = K \circ R_\omega,$$

where $R_\omega(\theta) = \theta + \omega$, with $\omega \in \mathbb{R}^n$.

- Anagolously, $\mathcal{K}$ is approximately invariant if

$$E := F \circ K - K \circ R_\omega,$$

where E is small in certain norm.

KAM theorem (a la Kolmogorov)

Let $\mathcal{K}$ be an approximately invariant torus satisfying certain non-degeneracy condition. Assume that the frequency ω satisfies certain non-resonance conditions. Then, if E is sufficiently small, there exists an invariant torus nearby.

The KAM Theorem

We present a quantitative version of [L-G-J-V,Nonlinearity,05]

See details in Chapter 4 of the survey: [C-F-H-L-M,Preprint,14].
Available at `http://www.maia.ub.es/~alex/review.pdf`

Let us consider an exact symplectic structure $\boldsymbol{\omega} = \mathrm{d}\boldsymbol{\alpha}$ on the n dimensional annulus, an exact symplectic map $F : \mathcal{A} \to \mathcal{A}$ homotopic to the identity and a frequency vector $\omega \in \mathbb{R}^n$. Let us assume that the following hypotheses hold:

Hypothesis 1: The map F, the 1-form $\boldsymbol{\alpha}$ and the 2-form $\boldsymbol{\omega}$ are real analytic and can be holomorphically extended to some complex strip $\mathcal{B}$ and continuously up to the boundary. Indeed, we have $\|\mathrm{D}F\|_{\mathcal{B}} \leq c_{F,1}$, $\left\|\mathrm{D}^2 F\right\|_{\mathcal{B}} \leq c_{F,2}$, $\|\Omega\|_{\mathcal{B}} \leq c_{\Omega,0}$, $\|\mathrm{D}\Omega\|_{\mathcal{B}} \leq c_{\Omega,1}$, $\|\mathrm{D}a\|_{\mathcal{B}} \leq c_{a,1}$ and $\left\|\mathrm{D}^2 a\right\|_{\mathcal{B}} \leq c_{a,2}$.

Hypothesis 2: There exists an approximately invariant torus $\mathcal{K}$ given by an embedding $K : \mathbb{T}^n \to \mathcal{A}$, homotopic to the zero section, satisfying

$$E(\theta) = F(K(\theta)) - K(\theta + \omega).$$

We assume that K can be holomorphically extended to $\mathbb{T}^n_\rho$, and continuously up to the boundary, for certain $\rho > 0$ and that

$$\|\mathrm{D}K\|_\rho < \sigma_L, \qquad \left\|\mathrm{D}K^\top\right\|_\rho < \sigma_L^*, \qquad \mathrm{dist}(K(\mathbb{T}^n_\rho), \partial\mathcal{B}) > 0.$$

Here, given two subsets $X, Y \in \mathbb{C}^{2n}$, we define their “distance” by

$$\mathrm{dist}(X, Y) = \inf\{|x - y|,\ x \in X,\ y \in Y\},$$

where $|\cdot|$ is the maximum norm.

Hypothesis 3: There exists a map $N^0 : \mathbb{T}^n \to \mathbb{R}^{2n\times n}$ that is real analytic and can be holomorphically extended to $\mathbb{T}^n_\rho$ and satisfies $\left\|N^0\right\|_\rho \leq c_{N^0}$, $\left\|(N^0)^\top\right\|_\rho \leq c^*_{N^0}$. Moreover $\mathrm{D}K$ and N^0 are transversal in the sense that they satisfy the geometrical non-degeneracy condition

$$\|B\|_\rho < \sigma_G, \qquad \left\|B^\top\right\|_\rho < \sigma^*_G,$$

where $B(\theta) = -(\mathrm{D}K(\theta)^\top \Omega(K(\theta))N^0(\theta))^{-1}$.

Hypothesis 4: The torsion matrix $T(\theta)$ satisfies the dynamical non-degeneracy condition $|\langle T\rangle^{-1}| < \sigma_T$.

Hypothesis 5: The frequency vector ω satisfies Diofantine conditions of type (γ, τ):

$$|k\cdot\omega - m| \geq \gamma\, |k|_1^{-\tau}, \qquad \forall k \in \mathbb{Z}^n \setminus \{0\},\ m \in \mathbb{Z},$$

where $|k|_1 = \sum_{i=1}^n |k_i|$.

THEN for every $0 < \rho_\infty < \rho$ there exist a constant $\hat{C}_*$ such that if the following condition holds

$$\frac{\hat{C}_* \|E\|_\rho}{\gamma^4 \rho^{4\tau}} < 1$$

then there exists a F-invariant torus $\mathcal{K}_\infty = K_\infty(\mathbb{T}^n)$, with the same frequency ω, analytic in $\mathbb{T}^n_{\rho_\infty}$, that satisfies

$$\|\mathrm{D}K_\infty\|_{\rho_\infty} < \sigma_L, \qquad \left\|\mathrm{D}K_\infty^\top\right\|_{\rho_\infty} < \sigma_L^*, \qquad \mathrm{dist}(K_\infty(\mathbb{T}^n_{\rho_\infty}), \partial\mathcal{B}) > 0.$$

Moreover, the torus $\mathcal{K}_\infty$ is close to the original approximation, in the sense that there exists a constant $\hat{C}_{**}$ such that

$$\|K_\infty - K\|_{\rho_\infty} \leq \frac{\hat{C}_{**}}{\gamma^2 \rho^{2\tau}} \|E\|_\rho \,. \qquad (1)$$

The constant $\hat{C}_*$

$$\rho = \frac{\delta}{a_3}, \qquad \delta_s = \frac{\delta}{a_1^s}, \qquad \rho_\infty = \frac{\rho}{a_2}, \qquad a_2 = 3\frac{a_1}{a_1 - 1}\frac{a_2}{a_2 - 1}.$$

First we show constants that control geometric objects. For example $\|T_K\|_\rho \leq c_T$. They can be improved depending on the problem, for example, $c_A = 0$ if $N^0(\theta)$ is Lagrangian.

$$\begin{aligned}
c_A &= \frac{1}{2}\sigma_B^* c_{N^0}^* c_{\Omega,0} c_{N^0} \sigma_B \\
c_N &= \sigma_L c_A + c_{N^0}\sigma_B \\
c_N^* &= c_A \sigma_L^* + \sigma_B^* c_{N^0}^* \\
c_P &= \sigma_L + c_N \\
c_P^* &= \max\{\sigma_L^*, c_N^*\} \\
c_T &= c_N^* c_{\Omega,0} c_{F,1} c_N
\end{aligned}$$

Intermediate bounds of the form $\frac{C_j}{\gamma^n \delta^{n\tau}} \|E\|_\rho$ that appear along the proof of the theorem.

$$
\begin{aligned}
C_1 &= \sigma_L^* \sigma_L c_{\Omega,1} \delta + n \sigma_L^* c_{\Omega,0} + 2n c_{\Omega,0} c_{F,1} \sigma_L \\
C_2 &= c_R C_1 \\
C_3 &= (1 + c_A) \max\{1, c_A\} C_2 \\
C_4 &= n c_N^* c_{\Omega,0} \gamma \delta^\tau + c_A C_2 \\
C_5 &= C_2 + n \sigma_L^* c_{\Omega,0} \gamma \delta^\tau \\
C_6 &= c_A C_2 + \sigma_L^* c_{\Omega,1} c_{F,1} c_N \gamma \delta^{\tau+1} + 2n c_{\Omega,0} c_{F,1} c_N \gamma \delta^\tau \\
C_7 &= \max\{C_4, C_5 + C_6\} \\
C_8 &= 2 c_R \sigma_L^* c_{\Omega,0} \\
C_9 &= C_8 + \sigma_T (c_N^* c_{\Omega,0} \gamma \delta^\tau + c_T C_8) \\
C_{10} &= c_R (c_N^* c_{\Omega,0} \gamma \delta^\tau + c_T (C_8 + C_9)) \\
C_{11} &= c_{N^0} \hat{C}_2(\sigma_L^*) c_{\Omega,1} \delta + 2n c_{\Omega,0}
\end{aligned}
$$

$$
\begin{aligned}
C_{11}^* &= c_{N^0}^* \hat{C}_2(\sigma_L) c_{\Omega,1} \delta + n c_{\Omega,0} \\
C_{12} &= \frac{1}{2} c_{N^0}^* c_{N^0} (\sigma_G^* c_{\Omega,0} \hat{C}_3 + \sigma_G^* c_{\Omega,1} \sigma_G \hat{C}_2 \delta + c_{\Omega,0} \sigma_G \hat{C}_3) \\
C_{13} &= \sigma_L C_{12} + n \hat{C}_2 c_A + c_{N^0} \hat{C}_3 \\
C_{13}^* &= \sigma_L^* C_{12} + 2n \hat{C}_2 c_A + c_{N^0}^* \hat{C}_3^* \\
C_{14} &= c_N^* c_N \hat{C}_2 (c_{\Omega,0} c_{F,2} + c_{\Omega,1} c_{F,1}) \delta + c_{\Omega,0} c_{F,1} (c_N^* C_{13} + c_N C_{13}^*) \\
C_{15} &= (C_3 + C_7) \max\{C_9 \gamma \delta^\tau, C_{10}\} + 2n c_{a,1} \gamma^3 \delta^{3\tau} + \frac{1}{2} c_{a,2} \gamma^3 \delta^{3\tau+1} \\
\hat{C}_2 &= \sigma_L C_{10} + c_N C_9 \gamma \delta^\tau \\
\hat{C}_3 &= 2 \sigma_G^2 C_{11} \\
\hat{C}_3^* &= 2 (\sigma_G^*)^2 C_{11}^* \\
\hat{C}_4 &= 2 \sigma_T^2 C_{14} \\
\hat{C}_5 &= 2 c_P C_{15} \gamma \delta^{\tau-1} + \frac{1}{2} c_{F,2} \hat{C}_2^2
\end{aligned}
$$

$$\hat{C}_6 = \max \left\{ \frac{n\hat{C}_2}{\sigma_L - \|\mathrm{D}K_0\|_{\rho_0}}, \frac{2n\hat{C}_2}{\sigma_L^* - \left\|\mathrm{D}K_0^\top\right\|_{\rho_0}}, \frac{\hat{C}_3}{\sigma_G - \|B_0\|_{\rho_0}}, \right.$$
$$\left. \frac{\hat{C}_3^*}{\sigma_G^* - \left\|B_0^\top\right\|_\rho}, \frac{\hat{C}_4}{\sigma_T - \left|\langle T_0\rangle^{-1}\right|} \right\}$$

$$\hat{C}_7 = \frac{\hat{C}_2\delta_0}{\mathrm{dist}(K_0(\mathbb{T}^n_{\rho_0}), \partial\mathcal{B})}$$

$$\hat{C}_8 = \max \left\{ 2C_3\gamma\delta_0^\tau, \frac{\hat{C}_6}{1 - a_1^{1-2\tau}}, \frac{\hat{C}_7}{1 - a_1^{-2\tau}} \right\}$$

... and finally

$$\hat{C}_* = \max \left\{ (a_1 a_3)^{4\tau} \hat{C}_5, (a_3)^{2\tau+1} \hat{C}_8 \gamma^2 \rho_0^{2\tau-1} \right\}$$
$$\hat{C}_{**} = a_3^{2\tau} \hat{C}_2 / (1 - a_1^{1-2\tau})$$

Numerical computations using the parameterization method

Given a periodic function f on $\mathbb{T}^n$, we consider a sample of points on the regular grid of size $N_\mathrm{F} = (N_{\mathrm{F},1}, \ldots, N_{\mathrm{F},n})$

$$\theta_j := (\theta_{j_1}, \ldots, \theta_{j_n}) = \left(\frac{j_1}{N_{\mathrm{F},1}}, \ldots, \frac{j_n}{N_{\mathrm{F},n}} \right),$$

where $j = (j_1, \ldots, j_n)$, with $0 \le j_l < N_{\mathrm{F},l}$ and $1 \le l \le n$. This defines an n- dimensional array $\{f_j\}$ with $f_j = f(\theta_j)$. The total number of points is given by $N_\mathrm{D} = N_{\mathrm{F},1} \cdots N_{\mathrm{F},n}$. The discrete Fourier transform (DFT) is

$$\{\hat{f}_k\} = \mathrm{DFT}(\{f_j\}), \qquad \text{with} \qquad \hat{f}_k = \frac{1}{N_\mathrm{D}} \sum_j f_j \mathrm{e}^{-2\pi \mathrm{i} k \cdot \theta_j},$$

where $k = (k_1, \ldots, k_n)$, with $0 \le k_l < N_{\mathrm{F},l}$ and $1 \le l \le n$. In particular, the average is given by

$$\hat{f}_0 = \langle \{f_j\} \rangle = \frac{1}{N_\mathrm{D}} \sum_j f_j.$$

Notice that DFT produces the interpolating trigonometric polynomial on the grid, that is,

$$f_j = f(\theta_j) = \sum_k \hat{f}_k \mathrm{e}^{2\pi \mathrm{i} k\cdot\theta_j},$$

and we denote $\{f_j\} = \mathrm{DFT}^{-1}(\{\hat{f}_k\})$. However, we emphasize that the right way to approximate functions in our context is by means of truncated Fourier series

$$f(\theta) \simeq \sum_k \hat{f}_k \mathrm{e}^{2\pi \mathrm{i} k'\cdot\theta},$$

where the multi-index $k' = (k'_1, \ldots, k'_n)$ is given as follows

$$k'_l = \begin{cases} k_l & \text{if } 0 \leq k_l < N_{\mathrm{F},l}/2 \\ k_l - N_{\mathrm{F},l} & \text{if } N_{\mathrm{F},l}/2 \leq k_l < N_{\mathrm{F},l} \end{cases}.$$

Of course, the truncated Fourier series coincides with the DFT on the points of the grid.

Given a periodic function f, discretized as $\{\hat{f}_k\}$, we compute the Fourier discretization of:

- a partial derivative $\partial_{\theta_l} f$

$$\{(\widehat{\partial_{\theta_l} f})_k\} = \{2\pi \mathrm{i} k'_l \hat{f}_k\},$$

- the composition $f \circ R_\omega$

$$\{(\widehat{f \circ R_\omega})_k\} = \{\mathrm{e}^{2\pi \mathrm{i} k' \cdot \omega} \hat{f}_k\},$$

- the solution $\mathcal{R}(f)$ of a one-bite cohomological equation

$$\{(\widehat{\mathcal{R}(f)})_k\}, \quad \text{where} \quad (\widehat{\mathcal{R}(f)})_k = \begin{cases} (1 - \mathrm{e}^{2\pi \mathrm{i} k' \cdot \omega})^{-1} \hat{f}_k & \text{if } k \neq 0 \\ 0 & \text{if } k = 0 \end{cases}.$$

Some features of our coding:

- It is very general: n, $\boldsymbol{\omega}$, $\boldsymbol{g}$, F, ω.
- We have used operator overloading introducing several classes in C++ (**complex**, **grid**, **matrix)**
- It uses arbitrary precision using **mpfr** or interval arithmetics using **mpfi**.

Example 1:

```
paramF=fft_F(paramR);
DparamF = diff(paramF);
DparamR = fft_B(DparamF);
```

Example 2:

```
GR = trans(LR)*MetricKR*LR;
BR = inv(GR);
NR = inv(MetricKR)*OmegaKR*LR*BR;
```

Some features of our coding:

- It is very general: n, $\boldsymbol{\omega}$, $\boldsymbol{g}$, F, ω.
- We have used operator overloading introducing several classes in C++ (**complex**, **grid**, **matrix)**
- It uses arbitrary precision using **mpfr** or interval arithmetics using **mpfi**.

Example 1:

```
paramF=fft_F(paramR);
DparamF = diff(paramF);
DparamR = fft_B(DparamF);
```

Example 2:

```
GR = trans(LR)*MetricKR*LR;
BR = inv(GR);
NR = inv(MetricKR)*OmegaKR*LR*BR;
```

Some features of our coding:

- It is very general: n, ω, $\boldsymbol{g}$, F, ω.
- We have used operator overloading introducing several classes in C++ (**complex**, **grid**, **matrix)**
- It uses arbitrary precision using **mpfr** or interval arithmetics using **mpfi**.

Example 1:

```
paramF=fft_F(paramR);
DparamF = diff(paramF);
DparamR = fft_B(DparamF);
```

Example 2:

```
GR = trans(LR)*MetricKR*LR;
BR = inv(GR);
NR = inv(MetricKR)*OmegaKR*LR*BR;
```

Direct application: golden curve of the standard map

For the standard map

$$\begin{array}{rcl} F_\varepsilon : \mathbb{T}\times\mathbb{R} & \longrightarrow & \mathbb{T}\times\mathbb{R} \\ (x,y) & \longmapsto & \left(x+y-\frac{\varepsilon}{2\pi}\sin(2\pi x),\, y-\frac{\varepsilon}{2\pi}\sin(2\pi x)\right), \end{array}$$

we have $\mathcal{A} = \mathbb{T}\times\mathbb{R}$, $\boldsymbol{\alpha} = y\,\mathrm{d}x$ and $\boldsymbol{\omega} = \mathrm{d}y\wedge\mathrm{d}x$.
For $\varepsilon = 0$ we have invariant tori parametrized by

$$K(\theta) = \begin{pmatrix}\theta\\ \omega\end{pmatrix}, \qquad \mathrm{D}K(\theta) = \begin{pmatrix}1\\ 0\end{pmatrix}, \qquad \omega = y.$$

From now on, we take $\omega = (\sqrt{5}-1)/2$.

ε	$\langle T \rangle$	$\nu_2(\varepsilon)$	$N_D/2$	E	E_{red}
0.1000	1.00052	4.609e–03	128	8.1e-13	3.5e-11
0.3000	1.00488	1.470e–02	128	3.5e-17	1.3e-14
0.5000	1.01487	2.913e–02	128	5.1e-17	1.9e-14
0.7000	1.03550	5.999e–02	128	4.7e-16	1.3e-13
0.9000	1.09828	2.503e–01	512	1.9e-16	2.9e-13
0.9100	1.10608	2.921e–01	512	4.4e-13	2.4e-10
0.9400	1.14190	5.762e–01	2048	4.1e-16	2.5e-12
0.9500	1.16310	8.465e–01	8192	7.8e-16	7.3e-12
0.9610	1.20412	1.732e+00	8192	1.5e-15	4.2e-11
0.9620	1.20995	1.913e+00	16384	2.2e-15	4.1e-11
0.9680	1.26930	5.095e+00	32768	2.6e-13	1.8e-09
0.9707	1.35709	1.988e+01	65536	7.2e-12	8.7e-08
0.9710	1.38321	2.930e+01	131072	1.7e-11	2.8e-07
0.9712	1.40923	4.278e+01	262144	3.8e-11	8.8e-07
0.9716	1.59494	5.292e+02	524288	7.2e-13	3.7e-07

Given a parameterization $K(\theta) = (\theta, 0) + (K_p^x(\theta), K_p^y(\theta))$, we consider the r-Sobolev seminorm of the periodic term of the x-variable

$$\nu_r(\varepsilon) := \|K_p^x\|_{H^r} = \frac{1}{(2\pi)^r}\|\mathrm{D}^r K_p^x\|_{L^2} = \sqrt{\sum_{k\in\mathbb{Z}} |k|^{2r}|\hat{K}_{p,k}^x|^2}.$$

Following renormalization group explanations, it turns out that there exists r_* such that for $r \geq r_*$ the seminorm $\nu_r(\varepsilon)$ blows up when $\varepsilon \to \varepsilon_c$. Moreover, the asymptotic behavior is of the form

$$\nu_r(\varepsilon) \simeq \frac{A_r}{(\varepsilon_c - \varepsilon)^{B_r}},$$

where the exponent satisfies the affine expression $B_r = a + br$, with $b \simeq 0.98740$

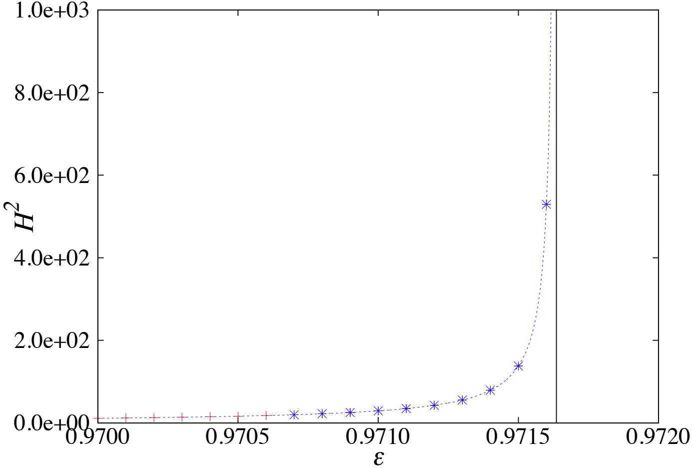

Figure: Blow up at the critical value of the Sobolev seminorm $\nu_2(\varepsilon)$.

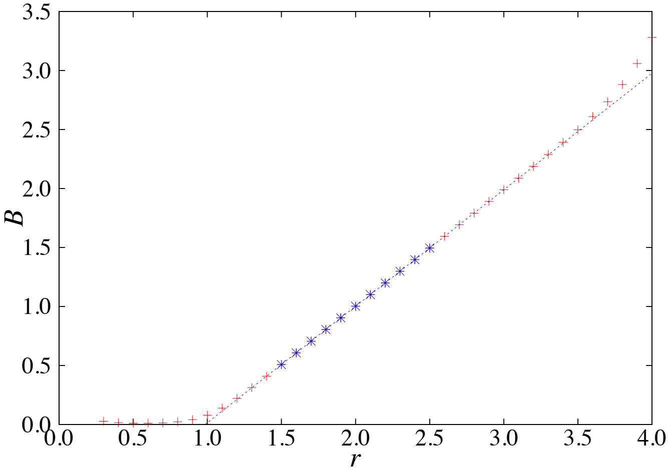

Figure: B_r versus r, and the corresponding linear fit.

$$B_r \simeq -0.9725247 + 0.9873479\, r.$$

r	ε_c	B_r
0.6	0.972458694072849	1.07393660804e-02
0.8	0.971776803592047	2.22475417451e-02
1.0	0.971655470476516	7.88917664257e-02
1.2	0.971637015679925	2.20418114383e-01
1.4	0.971635428344177	4.09909425520e-01
1.6	0.971635394237879	6.07181874296e-01
1.8	0.971635401206995	8.04751803217e-01
2.0	0.971635401069479	1.00223522858e+00
2.2	0.971635400427652	1.19966957378e+00
2.4	0.971635401868277	1.39706993308e+00
2.6	0.971635407308176	1.59445075775e+00
2.8	0.971635420401131	1.79186291341e+00
3.0	0.971635452115357	1.98951264953e+00
3.2	0.971635540433186	2.18822347324e+00
3.4	0.971635819315970	2.39117836419e+00
3.6	0.971636743093217	2.60996430744e+00
3.8	0.971639667321216	2.88091884546e+00
4.0	0.971647399558236	3.28055835189e+00

Table: Estimates of the critical value ε_c.

The CAP (with J.Ll. Figueras and A. Haro)

Given a parameterization K, approximately invariant, we define

$$\sigma_L = \|\mathrm{D}K\|_\rho \sigma, \qquad \sigma_L^* = \left\|\mathrm{D}K^\top\right\|_\rho \sigma, \qquad \sigma_G = \sigma^* = \|B\|_\rho \sigma,$$

with $\sigma > 1$. Similarly, we introduce

$$\sigma_T = |\langle T\rangle^{-1}|\sigma.$$

Hypothesis 1: In order to control the global objects we take $\mathcal{B} = \mathbb{T}_{\tilde\rho} \times \mathbb{C}$, with $\tilde\rho > \rho$, so that $K(\mathbb{T}_\rho) \subset \mathcal{B}$ and

$$\mathrm{dist}\left(K(\mathbb{T}_\rho), \partial\mathcal{B}\right) = \tilde\rho - \rho - \|K^x - \mathrm{id}\|_\rho .$$

The derivatives of F do not depend on y we can take an unbounded domain for this variable). We have

$$\|\mathrm{D}F\|_{\mathcal{B}} \leq c_{F,1} = 2 + \varepsilon \cosh(2\pi\tilde\rho),$$
$$\left\|\mathrm{D}^2 F\right\|_{\mathcal{B}} \leq c_{F,2} = 2\pi\varepsilon \cosh(2\pi\tilde\rho).$$

We also take $c_{\Omega,0} = 1$, $c_{\Omega,1} = 0$, $c_{a,1} = 1$ and $c_{a,2} = 0$.

Hypothesis 2: The initial parameterization satisfies the invariance equation up to an error

$$E(\theta) = \begin{pmatrix} K_p^x(\theta) + F_p^x(K(\theta)) - K_p^x(\theta+\omega) - \omega \\ F_p^y(K(\theta)) - K_p^y(\theta+\omega) \end{pmatrix},$$

for the standard map

$$E(\theta) = \begin{pmatrix} K_p^x(\theta) + \frac{\varepsilon}{2\pi}\sin(K^x(\theta)) - K_p^x(\theta+\omega) - \omega \\ \frac{\varepsilon}{2\pi}\sin(K^x(\theta)) - K_p^y(\theta+\omega) \end{pmatrix}.$$

Notice that the difficult part is $\sin(K^x(\theta))$ that contains infinitely many Fourier modes.

We have (at least) two choices

- Use Fourier models (let the PC do the hard work!)
- Resort to an analytic lemma (we avoid hard work by thinking)

Hypothesis 3: and so on ...

Hypothesis 2: The initial parameterization satisfies the invariance equation up to an error

$$E(\theta) = \begin{pmatrix} K_p^x(\theta) + F_p^x(K(\theta)) - K_p^x(\theta+\omega) - \omega \\ F_p^y(K(\theta)) - K_p^y(\theta+\omega) \end{pmatrix},$$

for the standard map

$$E(\theta) = \begin{pmatrix} K_p^x(\theta) + \frac{\varepsilon}{2\pi}\sin(K^x(\theta)) - K_p^x(\theta+\omega) - \omega \\ \frac{\varepsilon}{2\pi}\sin(K^x(\theta)) - K_p^y(\theta+\omega) \end{pmatrix}.$$

Notice that the difficult part is $\sin(K^x(\theta))$ that contains infinitely many Fourier modes.

We have (at least) two choices

- Use Fourier models (let the PC do the hard work!)
- Resort to an analytic lemma (we avoid hard work by thinking)

Hypothesis 3: and so on ...

Hypothesis 2: The initial parameterization satisfies the invariance equation up to an error

$$E(\theta) = \begin{pmatrix} K_p^x(\theta) + F_p^x(K(\theta)) - K_p^x(\theta+\omega) - \omega \\ F_p^y(K(\theta)) - K_p^y(\theta+\omega) \end{pmatrix},$$

for the standard map

$$E(\theta) = \begin{pmatrix} K_p^x(\theta) + \frac{\varepsilon}{2\pi}\sin(K^x(\theta)) - K_p^x(\theta+\omega) - \omega \\ \frac{\varepsilon}{2\pi}\sin(K^x(\theta)) - K_p^y(\theta+\omega) \end{pmatrix}.$$

Notice that the difficult part is $\sin(K^x(\theta))$ that contains infinitely many Fourier modes.

We have (at least) two choices

- Use Fourier models (let the PC do the hard work!)
- Resort to an analytic lemma (we avoid hard work by thinking)

Hypothesis 3: and so on ...

After some hours of straightforward (e infumables) computations...

$$\hat{C}_* = \max\left\{ \underbrace{(a_1 a_3)^{4\tau}\hat{C}_5}_{\hat{C}_{*,1}}, \underbrace{\frac{\sigma_*(a_3)^{2\tau+1}\gamma^2\rho^{2\tau-1}\hat{C}_2}{(\sigma-1)(1-a_1^{1-2\tau})}}_{\hat{C}_{*,2}}, \underbrace{\frac{(a_3)^{2\tau}\gamma^2\rho^{2\tau}\hat{C}_2}{(\tilde{\rho}-\rho-\|K^x-\mathrm{id}\|_\rho)(1-a_1^{-2\tau})}}_{\hat{C}_{*,3}} \right\}$$

$$\sigma_* = \max\left\{ \|\mathrm{D}K\|_\rho^{-1}, \left\|\mathrm{D}K^\top\right\|_\rho^{-1}, 4\|B\|_\rho \sigma^2, 16|\langle T\rangle^{-1}|\,\|B\|_\rho^3\sigma^5 \right\},$$

$$\hat{C}_5 = 4\gamma\delta^{\tau-1}\sigma\max\{C_4, C_5+C_6\}\max\{C_9\gamma\delta^\tau, C_{10}\} + 8\gamma^4\delta^{4\tau-1}\sigma + \frac{1}{2}c_{F,2}\hat{C}_2^2$$

$$\hat{C}_2 = \|\mathrm{D}K\|_\rho \sigma C_{10} + \|B\|_\rho \sigma\gamma\delta^\tau C_9$$

We have to select values of ρ, δ, σ, $\tilde{\rho}$ that satisfy

$$\frac{\hat{C}_* \|E\|_\rho}{\gamma^4 \rho^{4\tau}} < 1,$$

To reduce the number of parameters in this problem we consider two additional conditions. A suitable choice is to ask for $\hat{C}_{*,1} = \hat{C}_{*,2} = \hat{C}_{*,3}$.

- Assume that ρ is given (a possible initial choice is ρ such that $\exp(2\pi M\rho)$ saturates the precision).
- Given ρ, we move δ in a bounded set (depending on ρ).
- Given (ρ, δ) we obtain σ such that $\hat{C}_{*,1} = \hat{C}_{*,2}$ (by secant method).
- Given (ρ, δ, σ) we obtain $\tilde{\rho}$ such that $\hat{C}_{*,2} = \hat{C}_{*,3}$.

Step 1: computation with high precision

Using 8192 Fourier modes at most and arithmetic of 135 bits (around 40 digits) we obtain:

ε	N_{D}	E
0.10	128	9.4e-39
0.30	256	6.3e-37
0.50	512	1.3e-34
0.70	1024	2.7e-38
0.90	4096	1.0e-37
0.91	4096	1.2e-37
0.92	4096	7.7e-37
0.93	8192	1.9e-34
0.94	8192	2.4e-37

As we will see, we do not need such precision. But this will be good for illustration.

Step 2: Numerical verification of the KAM theorem

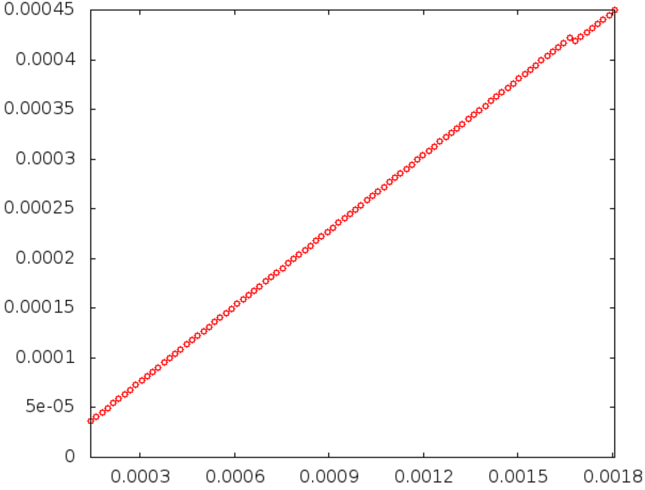

Figure: δ versus ρ for $\varepsilon = 0.94$.

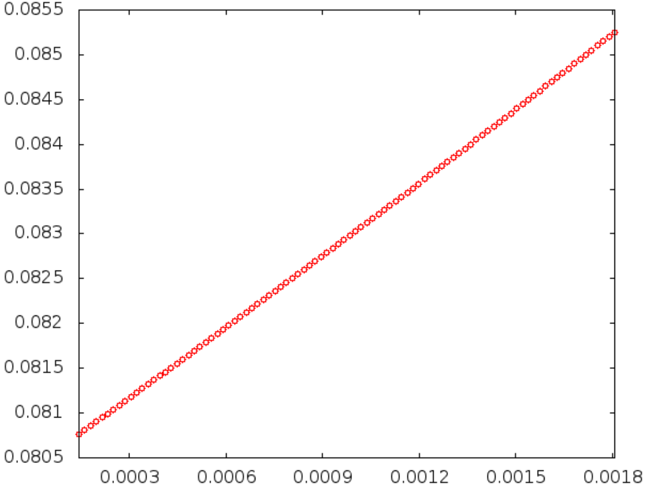

Figure: $\tilde{\rho}$ versus ρ for $\varepsilon = 0.94$.

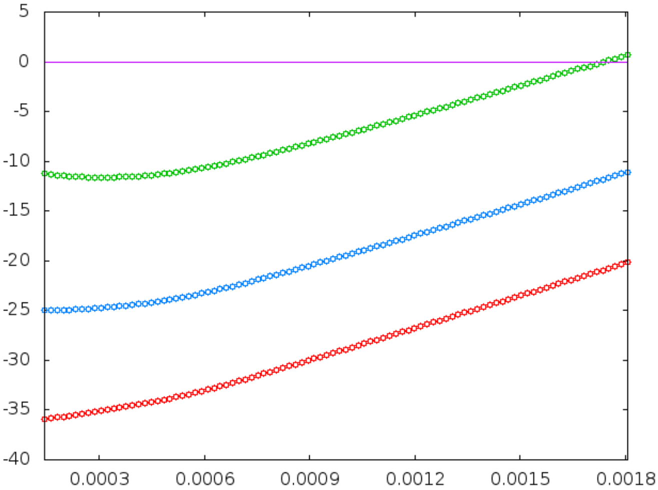

Figure: $\log_{10}$ of error, condition, correction versus ρ for $\varepsilon = 0.94$.

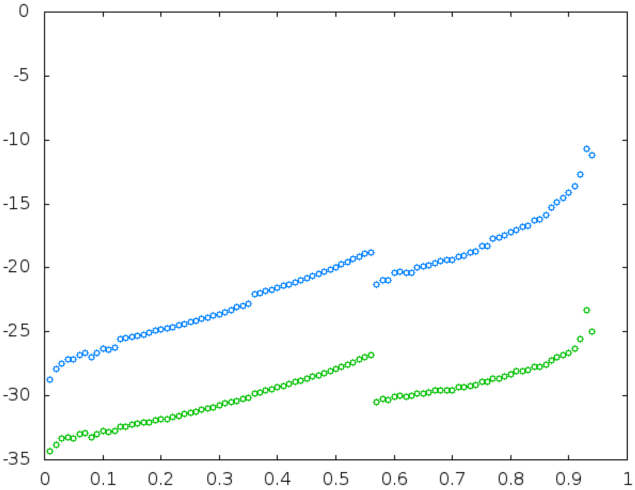

Figure: $\log_{10}$ of condition, correction versus ε.

Step 3: Rigorous evaluation of the error

Theorem: control of the norm $\|E\|_\rho$ for $n = 1$

Assume that F is analytic in $\mathcal{B}$ (the set containing the torus) and that K is a M-polynomial approximation of an invariant torus. Assume that $0 < \rho < \hat{\rho} < \tilde{\rho}$. Then

$$\|E\|_\rho \leq \sum_{k=0}^{M-1} |\hat{E}_k| \mathrm{e}^{2\pi|k'|\rho} + 2L \frac{\mathrm{e}^{\pi M(\rho-\hat{\rho})}}{1-\mathrm{e}^{2\pi(\rho-\hat{\rho})}} + 2L \frac{\mathrm{e}^{-2\pi M\hat{\rho}}}{1-\mathrm{e}^{-2\pi M\hat{\rho}}} \left(\frac{1-\mathrm{e}^{\pi M(\rho+\hat{\rho})}}{1-\mathrm{e}^{2\pi(\rho+\hat{\rho})}} + \frac{1-\mathrm{e}^{\pi M(\rho-\hat{\rho})}}{1-\mathrm{e}^{2\pi(\rho-\hat{\rho})}} \right)$$

where

$$\hat{E}_k = \frac{1}{M} \sum_{j=0}^{M-1} E(\theta_j) \mathrm{e}^{-2\pi \mathrm{i} kj/M}, \qquad L = \sup_{\hat{\rho}} |F(K(\theta))|.$$

The consequence is that the CAP has a cost $O(M \log(M))$.

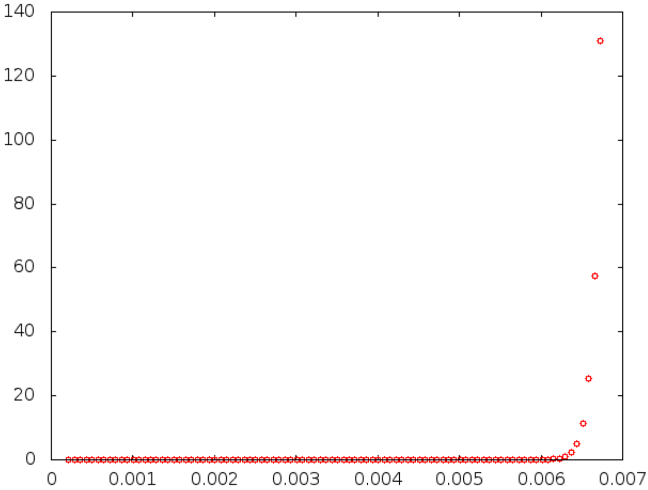

Figure: $\log_{10}(L)$ versus $\hat{\rho}$.

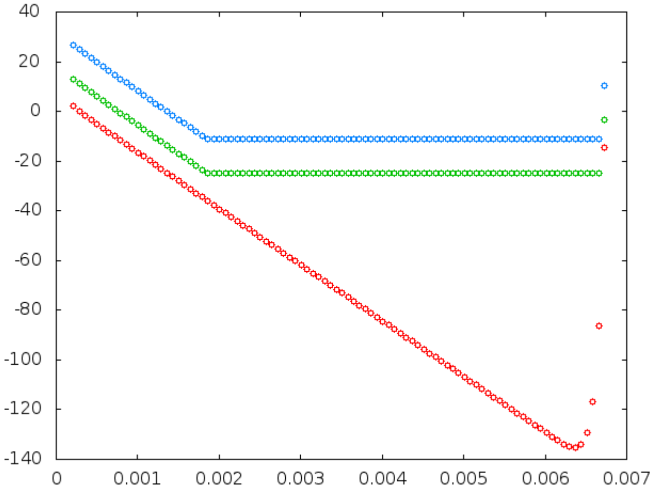

Figure: $\log_{10}$ of tail, condition, correction versus $\hat{\rho}$.

Conclusions and (near) future work

- We have presented a general KAM result with very sharp and explicit estimates for all the objects involved.
- The proof results in a fast an efficient numerical method to compute invariant tori that we have implemented in a very general and flexible way.
- Numerical computations can be rigorously validated using the KAM theorem. Preliminar computations on the golden curve of the standard map allows us to apply the theorem up to $\varepsilon < 0.9705$ with a reasonable effort (1.3 Gb of RAM). We expect[1] to obtain 0.9716. We know that for 0.9718 the curve does not exist.
- We plan to extend the CAP methodology to higher dimensions and consider more complex problems.
- We pretend to adapt the arguments to obtain estimates on the measure of invariant tori in phase space.

[1] P.D.: This value has been successfully obtained. See http://arxiv.org/abs/1601.00084